



## Deliverable D1.3.2 – PI-based assessments of 2 bladed concepts

Agreement n.:	308974
Duration	November 2012 – October 2017
Co-ordinator:	Danmarks Tekniske Universitet
Supported by:	



The research leading to these results has received funding from the European Community's Seventh Framework Programme FP7-ENERGY-2012-1-2STAGE under grant agreement No. 308974 (INNWIND.EU).

---

#### PROPRIETARY RIGHTS STATEMENT

This document contains information, which is proprietary to the "INNWIND.EU" Consortium. Neither this document nor the information contained herein shall be used, duplicated or communicated by any means to any third party, in whole or in parts, except with prior written consent of the "INNWIND.EU" consortium.

---

## Document information

<b>Document Name:</b>	Deliverable D1.3.2. – PI-based assessments of 2 bladed concepts
<b>Document Number:</b>	Deliverable D 1.32
<b>Author:</b>	Njomo Wilfried, Mahmood Mirzaei, Anand Natarajan, Frederik Zahle
<b>Document Type</b>	Report
<b>Dissemination level</b>	PU
<b>Review:</b>	Bernard Bulder
<b>Date:</b>	31.08.2015
<b>WP:</b>	WP 1
<b>Task:</b>	Task 1.3
<b>Approval:</b>	Approved by WP Leader

## 1 TABLE OF CONTENTS

<b>1</b>	<b>TABLE OF CONTENTS .....</b>	<b>3</b>
<b>2</b>	<b>INTRODUCTION .....</b>	<b>4</b>
<b>3</b>	<b>INNOVATIVE ROTOR CONTROL MECHANISMS (DTU).....</b>	<b>5</b>
3.1	Rotor design .....	5
3.2	Controller .....	7
3.3	Semi-floater concept.....	10
3.4	Natural frequency analysis .....	11
3.5	Characteristic curves .....	11
3.6	Design loads and sensors.....	13
3.7	Ultimate limit state.....	14
3.8	Fatigue limit state.....	16
3.9	Advantages of the semi-floater concept .....	19
<b>4</b>	<b>Conclusions.....</b>	<b>20</b>
	References.....	21

## 2 INTRODUCTION

Two rotors bladed rotors have the obvious advantage of reducing the number of blades to transport and possibly lower tower top mass as compared to 3 bladed rotors and thereby being able to thereby reduce the overall LCOE. However the key design frequency of a 2-bladed rotor is twice the rotational frequency, implying that the sampling of turbulence is reduced from 3 to 2 times the rotational frequency, and thus gives more fatigue load input to the tower. Further the jacket designed for the INNWIND.EU 10 MW reference turbine has a fundamental frequency of 0.29 Hz., which allows for significant 2p excitation just before the rotor reaches rated speed, since the variable speed region of the turbine is from [0.098 0.16] Hz. Increasing the support structure natural frequency will further complicate the problem, as this would now allow the second harmonic or 4P excitations from the rotor. Therefore in order to take advantage of the reduced tower top weight of a two bladed rotor, it is required to significantly reduce the natural frequency of the support structure to completely avoid 2p oscillations.

Enabling 2-bladed offshore wind turbines at 10 MW capacities as a viable design option allows radical design paradigm change for the offshore wind turbine industry, and will in turn support an emerging industrial development along these lines. In order for this to make a significant impact, the wind turbine should be installed at moderate water depths compatible with jackets. Therefore in this report, the reference wind turbine water depth of 50m is used in the design of the 2-bladed offshore wind turbine. This ambition can be summed up as moving the 2-bladed large offshore wind turbine concept from TRL level 2 to 3, that is a full design of the 2 bladed offshore turbine at 10 MW can be made, which is principle is ready to be tested at a lab scale.

This is achievable by using innovative sub structure design concepts where the fundamental frequency of the structure is below the 2P frequency at cut-in, that is below 0.19 Hz. and also below the fundamental wave excitation frequency. The peak spectral frequency of waves is usually between 0.1 Hz to 0.2 Hz. and therefore, if the fundamental frequency of the support structure is below 0.1 Hz., then it satisfies both objectives, i.e., it is below the 2P excitation frequency and below the wave excitation frequency. However usually, such low sub structure natural frequencies are only possible for floating foundations, which have other design constraints, such as they can be installed in deep waters above 100m etc. However in Task 4.1 of the INNWIND.EU project in deliverable 4.12, an innovative foundation was proposed, namely a semi floater, which is anchored to the soil, but only constrained in translator motion by a universal joint. The rotary movements are arrested by means of a buoyancy chamber and by mooring lines. This semi floater is designed at 50m water depth and presents an alternative solution to the jacket. A detailed design of the semi floater with mooring lines and universal joint is presented in deliverable D4.13.

This Semi floater foundation concept from D4.13 is herein used as the support structure for the 2 bladed rotor developed in WP2, deliverable D2.11. However the turbine is used as an upwind concept instead of a downwind concept as done in D2.11 to allow the same sub structure from WP4 to be used. This allows the design and integration of multiple innovations developed in the INNWIND.EU project and presents a fully innovative wind turbine concept at the 10 MW scale. The overall innovative concept of mounting an integrated two-bladed rotor designed for reduced head weight and reduced loads onto a novel offshore support structure suitable for moderate water depths has not been investigated before. No large scale two-bladed offshore wind turbines have been installed today and therefore this proposed design will leverage state-of-the-art design tools and component designs already developed to quantify the 2-blade wind turbine performance and verify the concept's viability. Suggestions for further optimizing the performance of the system for reduced loads and longer life through active controls is also made.

Since the rotor design and the semi floater design are explained in D2.11 and D4.12, D.13 respectively, the focus in this report will be more on the integrated turbine and its performance as quantified by fully coupled aero-hydro-elastic simulations.

### 3 INNOVATIVE ROTOR CONTROL MECHANISMS (DTU)

The DTU reference wind turbine of 10 MW [3-01] is converted into a two-bladed version and is placed in a 50 m water depth. Due to load excitation, two-bladed wind turbines perform poorly when mounted on traditional fixed support structures like monopile or jacket. The semi-floater concept as introduced by Refs [3-02] and [3-03] and later designed in further details by Ref [3-04] is used as foundation.

New blade is designed for the two-bladed wind turbine which is explained in the section on rotor design. As for the controller structure we have kept the same structure as the three-bladed turbine. The two-bladed rotor is modeled in HAWCStab2 for aero-elastic stability analysis, aerodynamic gradient calculations and also for automatic tuning of the controllers. The  $C_p$  and  $C_t$  of the two-bladed are also obtained using HAWCStab2 for steady state analysis of the turbine as well as model-based controller design. This report also presents load prediction and general behavior of the system.

#### 3.1 Rotor design

The most important part of the conversion of a three-bladed rotor to a two-bladed rotor is to keep a constant solidity by scaling the blade chord by a factor of 1.5. The overall performance of the two-bladed is similar to the three-bladed except for the tip loss effect [3-010]. The tip loss effect is slightly higher for the two-bladed turbine [3-011], [3-013] and [3-014]. Figure below shows a comparison of the chord length of the two-bladed and the three-bladed turbine along the blade.

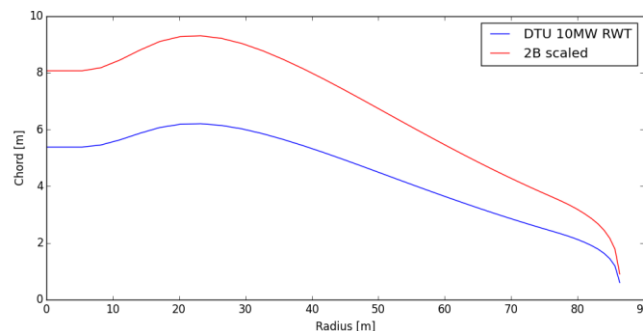


Figure 3.1-1 Chord of the blades

Using the same blade solidity by adjusting for the chord length enables the use of the original collective pitch controller for power regulation. The tuning of the controller is explained in the next section. The up-wind configuration of turbine is also kept. The twist and relative thickness of the blade are also the same as the three-bladed turbine, as seen in figures below:

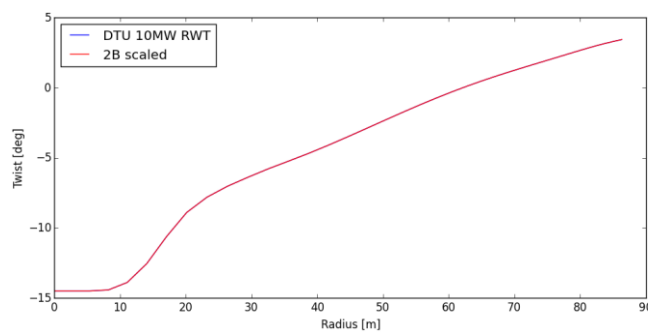


Figure 3.1-2 Twist of the blades

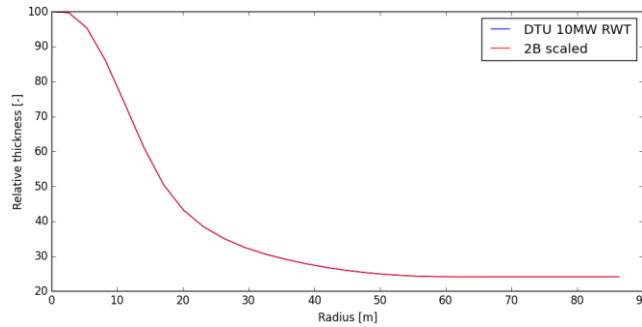


Figure 3.1-3 Relative thickness of the blades

The calculation of the stiffness and mass of the blade is taken from [3-011] and mentioned here for ease of access. Since the blade chord is scaled by a factor of 1.5 the stiffness properties also change accordingly. If we assume that the blade is built with a main spar as illustrated in Figure 3.1-4 the section modulus is roughly speaking proportional to the thickness, height and width of the spar.

$$I = \frac{1}{12}(bh^3 - b_i h_i^3) \quad (1)$$

Replacing  $b_i$  with  $b-2t$  and  $h_i$  with  $h-2t$  and ignoring all terms with higher order power terms of  $t$  leads to

$$I \approx \frac{1}{2}bh^2t + \frac{1}{6}h^3t \quad (2)$$

and the corresponding section modulus  $W$

$$w = \frac{I}{0.5h} \approx bht + \frac{1}{3}h^2t \quad (3)$$

We assume that the blade loads increases with the scale factor of 1.5, so the two-bladed load  $L_{2B}$  equals  $1.5 L_{3B}$  and we want to scale the blade thickness so the material stress remains constant.

$$\frac{\sigma_{3b}}{\sigma_{2b}} \equiv 1 \Rightarrow \frac{L_{3B}W_{2B}}{L_{2B}W_{3B}} \equiv 1 \quad (4)$$

Combining the last two equations and the scale factor of 1.5 on the load  $L_{2B}$ , width  $b_{2B}$  and height  $h_{2B}$  leads to

$$t_{2B} = 0.667t_{3B} \quad (5)$$

The cross section weight is proportional to the area

$$\frac{A_{2B}}{A_{3B}} = \frac{2(b_{2B} + h_{2B})t_{2B}}{2(b_{3B} + h_{3B})t_{3B}} \quad (6)$$

Inserting the factor of 1.5 on  $b_{2B}$ ,  $h_{2B}$  and the factor of 0.667 on  $t_{2B}$  leads to

$$A_{2B} = A_{3B} \quad (7)$$

This means that the overall weight of one blade for the two-bladed turbine is identical to one blade for the three-bladed turbine.

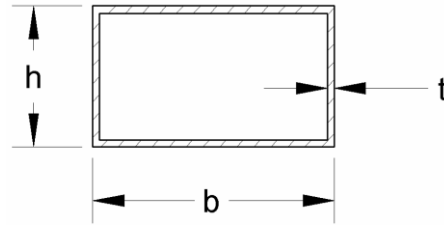


Figure 3.1-4 cross section of the main spar of the blade (Larsen, et al., 2007)

Using the blade design explained above the two-bladed rotor system is modeled in HAWCStab2 [3-08] for further stability analysis and controller design. The quasi-steady  $C_p$  and  $C_t$  curve of the rotor are also obtained for steady state analysis and design of model based controllers. The figure below shows the  $C_p$  curve of the two-bladed wind turbine. The power performance is therefore optimized by controller  $C_p$ -tip speed ratio tuning as shown in Fig. 3.1.

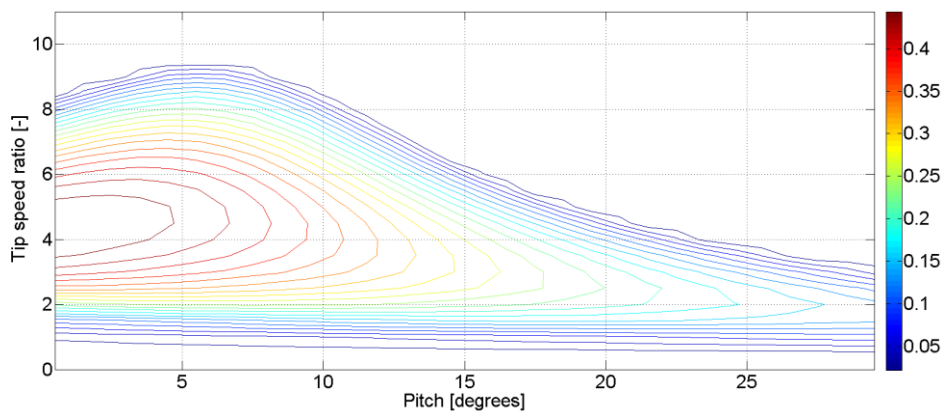


Figure 3-1 -  $C_p$  curve of the two bladed wind turbine

## 3.2 Controller

The controller has the same configuration as the three-bladed wind turbine [3-07]. In this configuration there are different controllers that are responsible for different operating regimes. There is a partial load controller that makes sure the wind turbine is producing maximum power for wind speeds below rated. This controller basically adjusts the rotational speed of the turbine to using the generator torque to maintain a constant and optimal tip speed ratio. In the partial load region the collective pitch of the blades is kept constant and at its optimal value. This means the rotational speed of the rotor should be adjusted as a linear function of the wind speed. This is done through a controller called  $K - \omega$ . Following the optimum tip speed ratio cannot hold in the entire partial load region as the rotational speed of the wind turbine is constraint from below by the minimum rotational speed and from above by the rated rotational speed. For these cases a PI controller that regulates the rotational speed using the generator torque is employed.

As for the full load region, there is another controller that regulates the rotational speed and power using collective pitch of the blades and the generator torque. We retuned the parameters of the partial load and the full load controllers for the new rotor configuration. The following sections give a detailed analysis of the tuned parameters.

### The partial load controller

As mentioned before, the objective of the partial load controller is to maximize the produced power when the wind speed is below the rated value. In this region the generator torque is determined by a simple  $K - \omega$  controller as long as the rotational speed is not limited to its minimum or rated

value. When the rotational speed is limited from below by the minimum value and from above by the rated value, the PI torque controller is activated and maintains a constant rotational speed by adjusting the generator re-action torque. Table below shows a list of parameters in the DTU controller for the partial load region.

**Table 3-1 - Partial load control parameters**

Parameters	Units
Optimal Cp tracking K factor	[kNm/(rad/s) <sup>2</sup> ]
Proportional gain of torque controller	[Nm/(rad/s)]
Integral gain of torque controller	[Nm/rad]
Differential gain of torque controller	[Nm/(rad/s <sup>2</sup> )]

For the partial load controller, the  $K$  value in the  $K - \omega$  controller is re-calculated based on the  $C_p$  curve of the two-bladed rotor configuration. The  $C_p$  curve is calculated using HAWCStab2 and the  $K$  coefficient of the torque controller:

$$Q_g = K\omega^2 \quad (8)$$

is calculated as:

$$K = \frac{1}{2} \eta \rho A C_{p_{opt}} R^3 / \lambda_{opt}^3 \quad (9)$$

in which Therefore,  $\eta$  is the efficiency of the turbine,  $\rho$  is the air density,  $A$  is the rotor area,  $C_{p_{opt}}$  is the optimum value of the  $C_p$  curve,  $\lambda_{opt}$  is the optimum value of the tip speed ratio and  $R$  is the rotor radius. The other values, namely proportional, integral and derivative gains of the torque controller are kept the same as the three-bladed wind turbine.

### The full load controller

The objective of the full load controller is to regulate the rotational speed and the generated power around their respective rated values. This is achieved with a controller that adjusts the pitch of the blades to maintain a constant aerodynamic power and the generator reaction torque to keep the generated power constant. The pitch controller is a gain scheduled PI controller that traditionally reacts on the rotational speed error. However in the DTU controller it is a PI controller based on combined rotational speed and generated power errors. The speed error is obtained as the difference between the second order low-pass filtered low speed shaft generator speed and the rated speed. The power error is the difference between the reference power  $P_{ref}$  and the rated power  $P_0$ . Both errors are notch filtered around the frequency specified by the user as the free-free drivetrain frequency. This frequency is assumed to be constant although HAWCStab2 eigenvalue analysis often shows a small variation with operational point (as a result wind speed variations). Note that both errors contribute to the same proportional term  $\theta_{p,k}$  and same integral term  $\theta_{i,k}$ . The latter is important because it ensures that the reference pitch angle is kept at the minimum pitch angle until rated power is reached; assuming that the right weighting between the integral speed error gain  $K_I$  and power error gain  $K_p^I$  has been selected by the user.

The generated power can be derived as  $P_e = Q_g \times \omega_g$ , in which  $Q_g$  is the generator torque and  $\omega_g$  is the rotational speed of the generator. Based on the power control strategy we can either keep the generated power constant by adjusting the generator torque or keep the generator torque constant. In this work we have used the former strategy namely keeping the generated power constant by adjusting the generator torque in response to the variations in the rotational speed. For the full load region the parameters to be tuned are the following:

Table 3-2 - Full load control parameters

Parameters	Units
Generator control switch	[1=constant power, 2=constant torque]
Proportional gain of pitch controller	[rad/(rad/s)]
Integral gain of pitch controller	[rad/rad]
Differential gain of pitch controller	[rad/(rad/s <sup>2</sup> )]
Proportional power error gain	[rad/W]
Integral power error gain	[rad/(Ws)]
Coefficient of linear term in aerodynamic gain scheduling, KK1	[deg]
Coefficient of quadratic term in aerodynamic gain scheduling, KK2	[deg <sup>2</sup> ]
Relative speed for double nonlinear gain	[-]

As mentioned before the constant power strategy is chosen in this work and therefore the generator control switch is set to be 1. The proportional and integral pitch gains are tuned using HAWCStab2. In this method the frequency and damping of the regulator mode of the closed loop system is given to HAWCStab2 and the program automatically calculates the parameters of the PI controller,  $K_p$  and  $K_i$ . In order to avoid excitation of the natural modes of the wind turbine structure, the regulator mode frequency should be less than the lowest eigen-frequency of the turbine. In the case of the semi-floating wind turbine, the slowest dynamic of the system is the tower fore-aft mode (which has almost the same frequency as the tower side-side mode). Thereafter we used a brute force method to fine tune controller parameters. In this method, we ran different simulation cases of steps in wind speed on a grid of different values of  $K_p$  and  $K_i$  and chose the values that give the minimum total variation (TV) [3-012] in the rotational speed response. HAWCStab2 also calculates the gain scheduling coefficient gains KK1 and KK2 based on the aerodynamic gradient of the rotor.

Figures below show the performance of the controller for wind steps from 5 m/s to 25 m/s. The figures include collective pitch of the blades, the rotational speed of the rotor and the generated power.

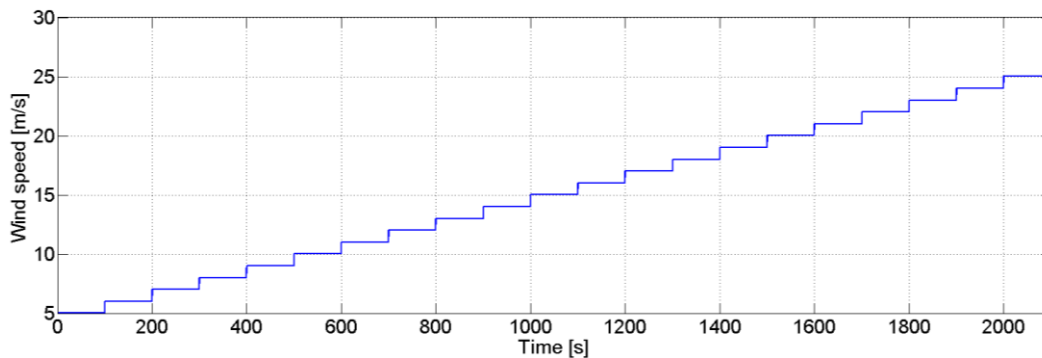


Figure 3.2-1 - Wind speed steps from 5m/s to 25m/s

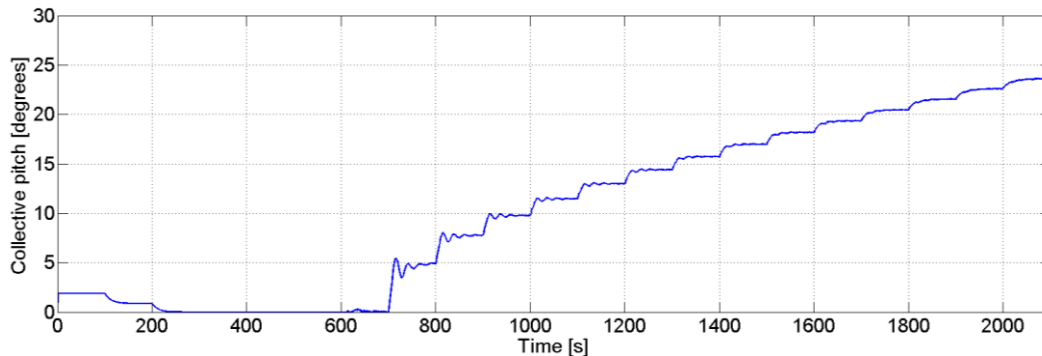


Figure 3.2-2 - Collective pitch of the blades

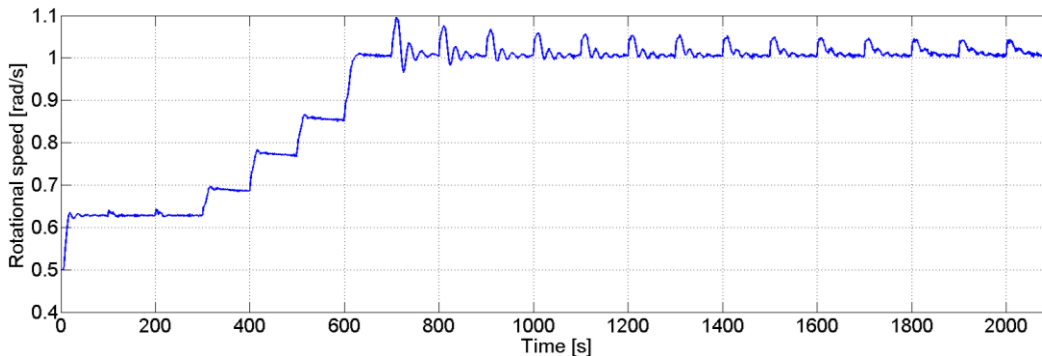


Figure 3.2-3 - Rotational speed of the rotor

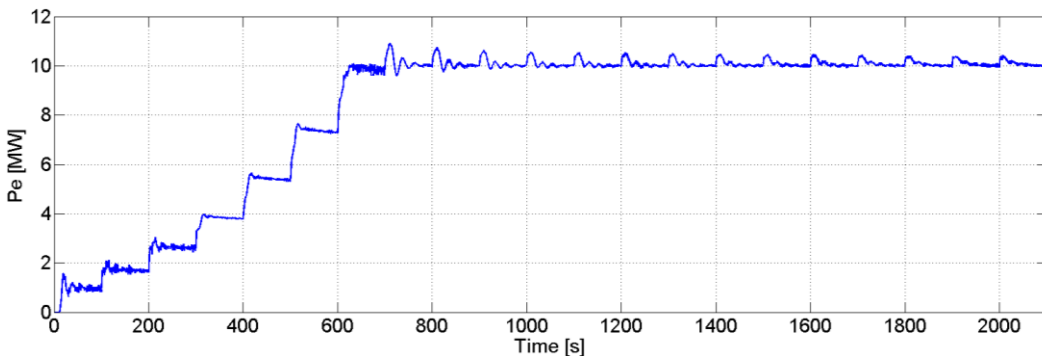


Figure 3.2-4 - Generated power

### 3.3 Semi-floater concept

The semi-floater concept has been thoroughly described in Refs [3-02] and [3-03]. It is primarily made of a floating system, a mooring system, and a universal joint mounted on a reinforced concrete base placed at seabed. The floating system is a set of floating cylinder, buoyant chamber, and ballast. The mooring system consists of 6 lines anchored to the seabed and connected to the buoyant chamber through delta connections. Ref [3-04] presents a detailed design of the concept; it provides information about material properties and geometry (Figure 3.3-1).

The mooring and floating systems have been integrally modelled in the computer software package HAWC2 [3-05], whereas the universal joint has been modeled in HAWC2 as

superelement with equivalent stiffness, damping and mass matrices. Simulations have been carried out during 600 s each.

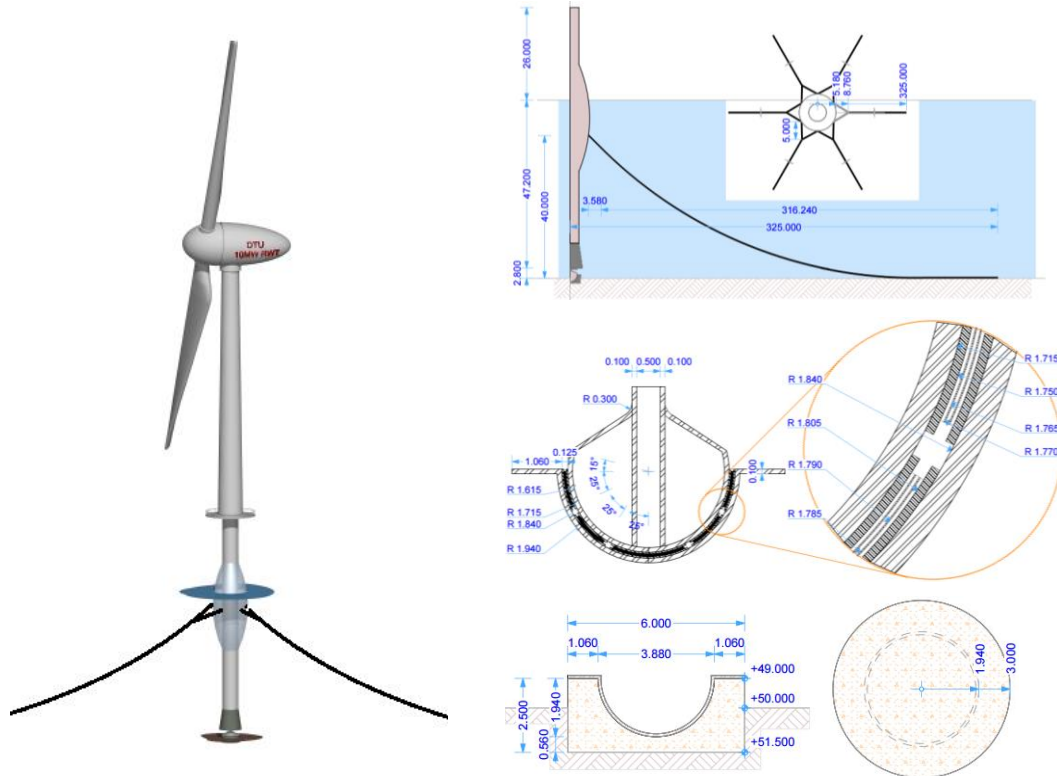


Figure 3.3-1 – Semi-floater concept

### 3.4 Natural frequency analysis

Modal analyses have been performed on the overall structure at stand-still position. Table 3-3 shows the natural frequencies and the logarithm decrement of the whole structure. The first tower modes have natural frequencies at about 0.068 Hz, which is out of the 1P excitation range, [0.10 Hz, 0.16 Hz], and is at the lower tail of the wave spectrum (lower than 3% of the wave energy during production phase).

Table 3-3 – Overall structure's natural frequency

Mode	Natural frequency [Hz]	Logarithmic Damping [%]
1st Tower side-side mode	0.0679	12.713
1st Tower fore-aft mode	0.0680	12.734
1st fix-free mode	0.0751	0.0059
1st Tower yaw mode	0.1516	0.0544

### 3.5 Characteristic curves

Four characteristic curves have been selected to depict the global performance of the structure: power curve, thrust force curve, rotor rotational speed curve and blade pitch angle curve. They are obtained by applying a steady wind, which linearly increases from 4 m/s to 25 m/s during 2500 s. Sea states are set as those for 15 m/s wind speed. Each of these curves (Figure 3.5-1 to Figure 3.5-4) is compared to their respective parents from DTU RWT 10 MW. Insignificant deviations are found between the two cases, revealing an acceptable performance of the two-bladed system.

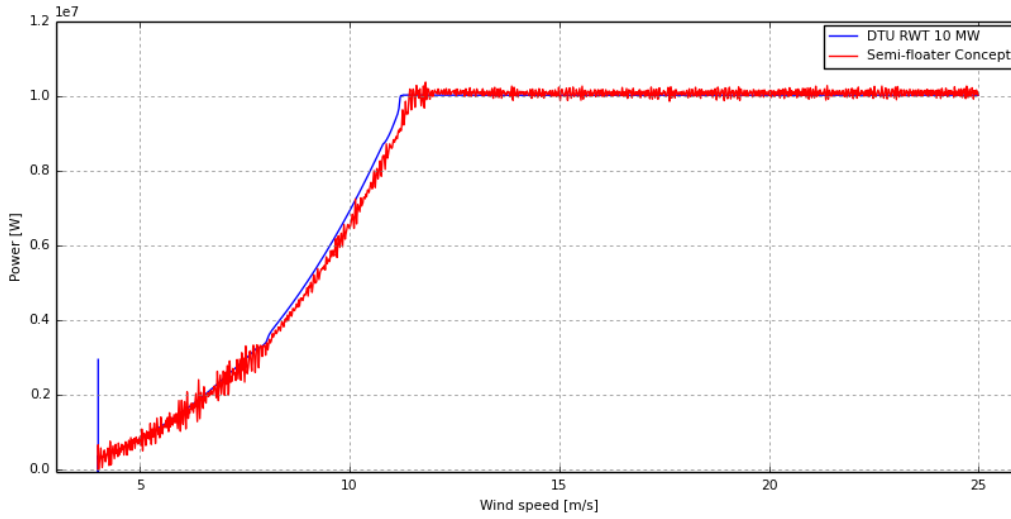


Figure 3.5-1 – Generated power curve

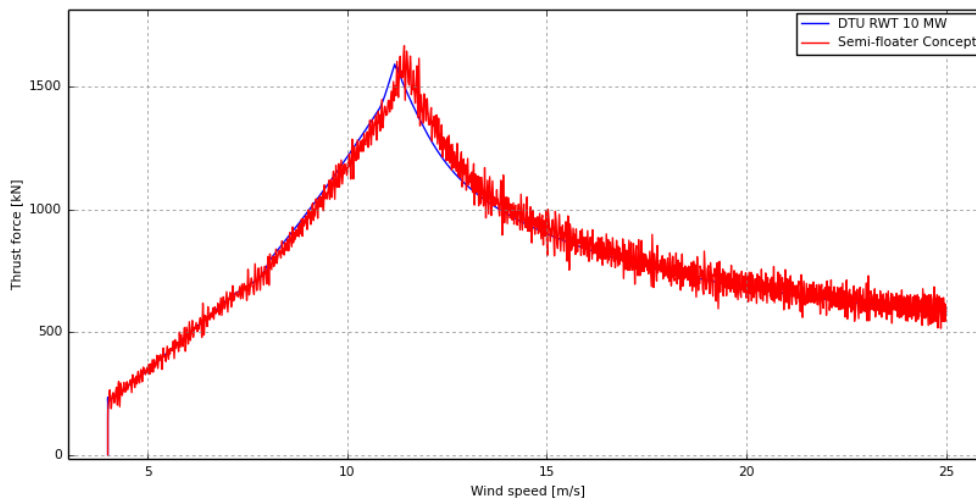


Figure 3.5-2 – Thrust force curve

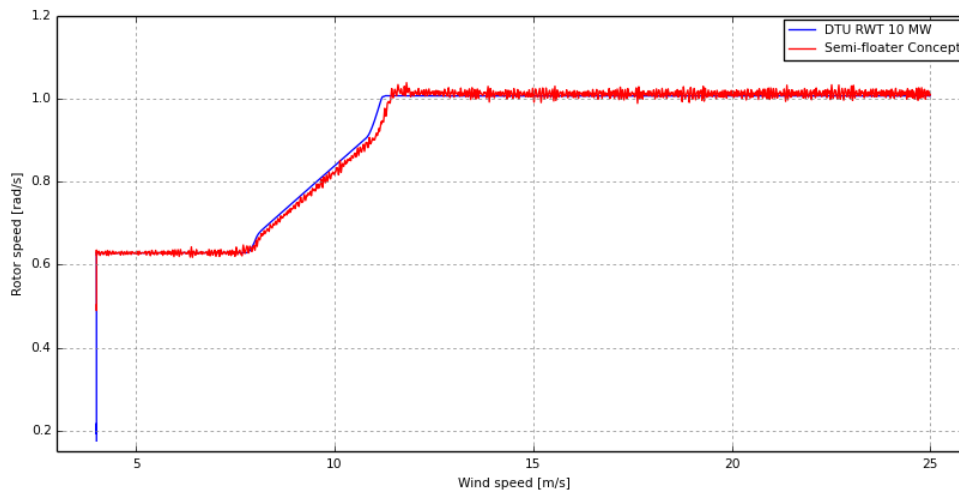


Figure 3.5-3 – Rotor rotational speed curve

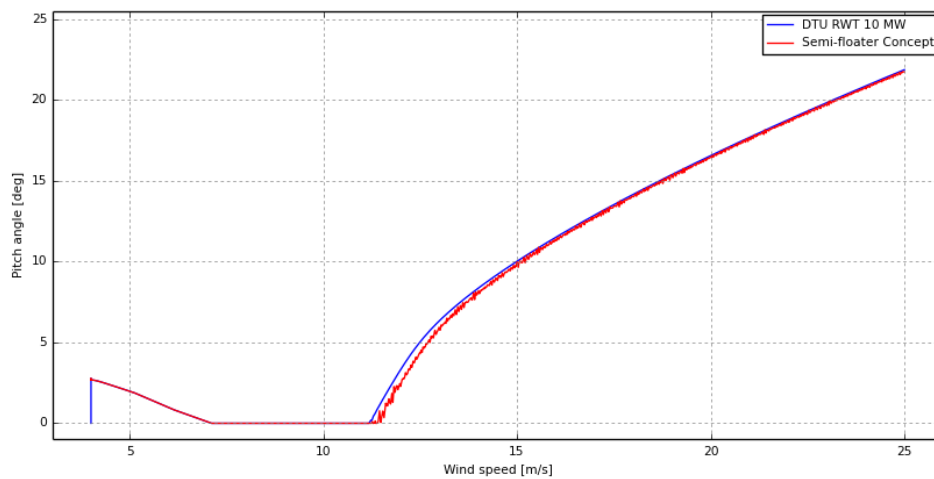


Figure 3.5-4 – Blade pitch curve

### 3.6 Design loads and sensors

Two design load cases as defined by IEC 61400-3 [3-06] are considered: 1.2 for fatigue limit state, and 1.3 for ultimate limit state.

DLC 1.2: 11 wind speed bins (5 m/s, 7 m/s, 9 m/s, 11 m/s, 13 m/s, 15 m/s, 17 m/s, 19 m/s, 21 m/s, 23 m/s, 25 m/s) with six wind seeds each have been applied each with yaw errors  $\pm 10^\circ$  from the normal to the rotor plane. Pierson-Moskowitz waves were misaligned to wind direction by  $\pm 10^\circ$ . That makes  $11 \times 6 \times 3 \times 3 = 594$  scenarios.

DLC 1.3: six wind seeds for each of 11 wind speed bins have been applied each with no yaw error. Waves of JONSWAP type were aligned along wind direction. That makes  $11 \times 6 = 66$  scenarios.

Atmospheric conditions and sea states are assumed to follow those of Ref [3-07] with the same occurrence distribution as summarized in Table 3-4.

In order to present load results, three structural locations have been chosen. They are tower top, tower base and joint top. At each of these locations, six loads (three forces and three moments) are collected.

**Table 3-4 – Meteocean conditions (adapted from Ref [3-07])**

Wind speed [m/s]	Turbulence Intensity [%]	Significant height, Hs [m]	Peak period, Tp [s]	Occurrence [hrs/yr]
5	18.95	1.14	5.82	933.75
7	16.75	1.245	5.715	1087.3
9	15.6	1.395	5.705	1129.05
11	14.9	1.59	5.81	1106.75
13	14.4	1.805	5.975	1006.4
15	14.05	2.05	6.22	820.15
17	13.75	2.33	6.54	633
19	13.5	2.615	6.85	418.65
21	13.35	2.925	7.195	312.7
23	13.2	3.255	7.6	209.9
25	13	3.6	7.95	48.9612
42.73	11.00	9.400	13.700	-

### 3.7 Ultimate limit state

Interface offsets are defined as the shift of the interface in its plane. In other words, they are the combination of surge and sway. During the production regime (DLC 1.3), mean and maximum averages of 1.97 m and 3.56 m have been respectively obtained for the interface offsets. These averages correspond to tower tilt angle of 1.48 deg and 2.68 deg, respectively. Individual values for each wind speed bin are depicted in Figure 3.7-1. The maxima of the interface offsets are obtained for wind speed around 13 m/s to 15 m/s, which is a bit higher than the rated wind speed 11.4 m/s.

The tilt angles observed lie within the lower end of the acceptable ranges for floating structures. A consequence is the slight oscillation of characteristic curves around their respective mean values. Similarly, maximum, mean, and minimum loads (forces and moments) are presented with respect to each wind speed bin at the handled structural locations. Side-side force, vertical force, and yaw moment consistently oscillate around constant mean value. At tower top and interface, fore-aft forces and moments present a bump or attain their maxima around the rated wind speed.

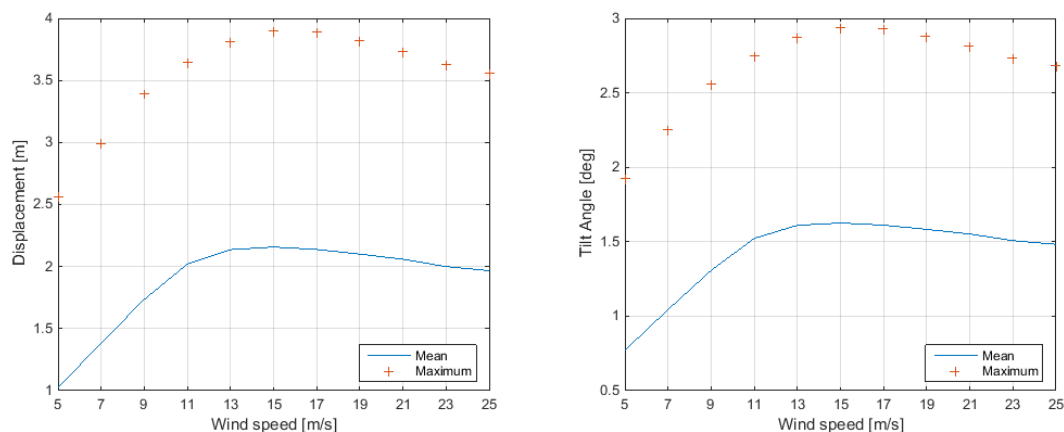


**Figure 3.7-1 – Interface offset and tower tilt angle**

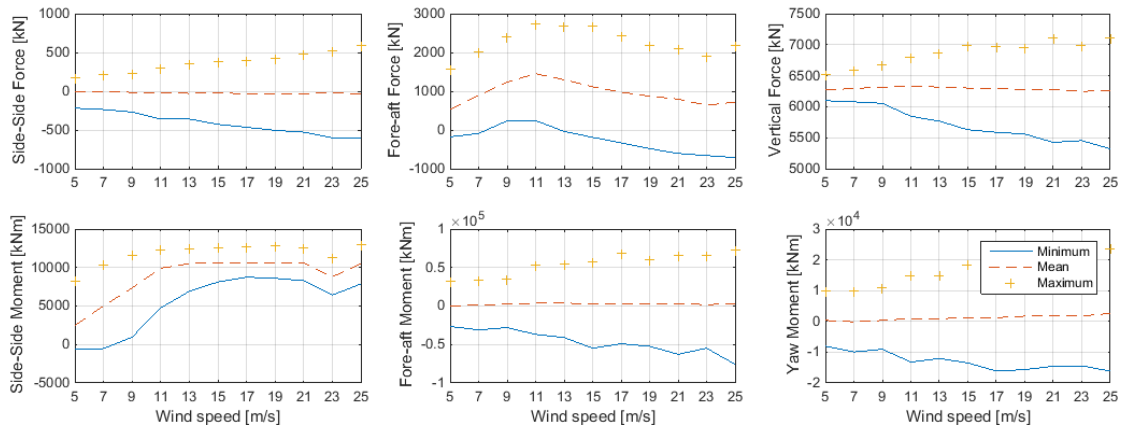


Figure 3.7-2 – Ultimate loads at tower top

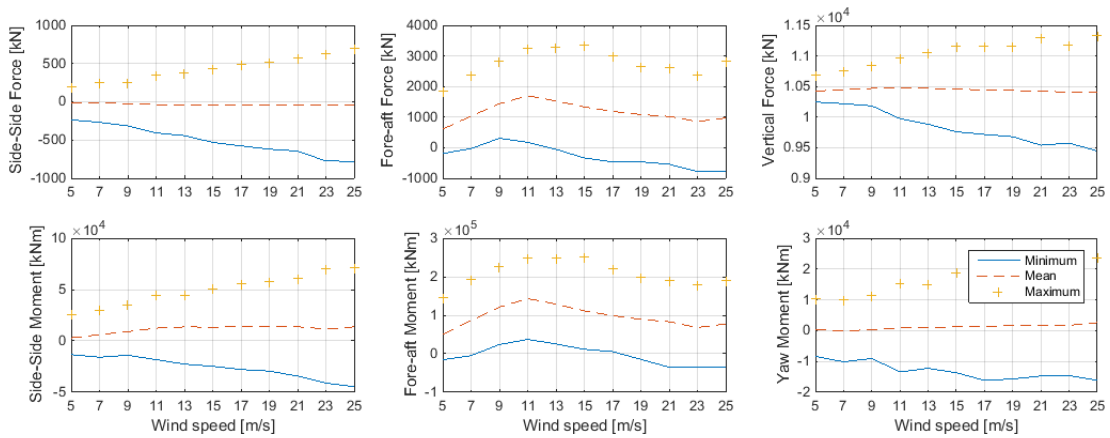


Figure 3.7-3 – Ultimate loads at interface

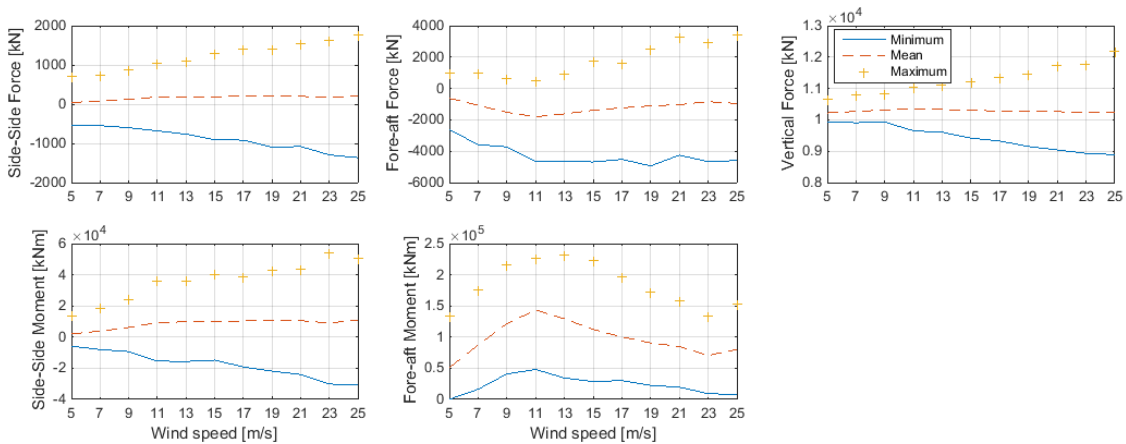


Figure 3.7-4 – Ultimate loads at joint top

### 3.8 Fatigue limit state

For a lifetime of 25 years, equivalent damage loads have been computed at the three structural locations selected above. Table 3-5 collects these loads for the respective six directions. The equivalent damage loads have been obtained by:

$$S_L = \left( \frac{\sum_i t_i \sum_j n_{ij} S_{ij}^m}{N_{eq} T_s} \right)^{1/m}, \quad (10)$$

where

- $m = 4$  is the Wohler factor;
- $N_{eq} = 10^7$  is the equivalent number of cycles during lifetime;
- $T_s = 10 \text{ min} = 600 \text{ s}$  is the simulation duration;
- $t_i$ : is the occurrence of a scenario,  $i$  in 25 years;
- $S_{ij}$ : is the load range,  $j$  for scenario,  $i$  as obtained from rainflow counting;
- $n_{ij}$ : is the number of cycles of load range bin,  $j$  for scenario,  $i$ .

**Table 3-5 – Damage equivalent loads for 25 years**

	Fx [kN]	Fy [kN]	Fz [kN]	Mx [kNm]	My [kNm]	Mz [kNm]
Tower top	616.2	1870.2	1232.4	82518.0	4112.1	17866.0
Interface	775.8	2484.4	1336.6	127830.0	57021.0	17549.0
Joint Top	1758.4	4596.1	2106.9	86718.0	32680.0	-

The INN WIND jacket [3-012] is chosen as benchmark as it is designed under comparable conditions. In particular, the equivalent fatigue loads at interface are compared with those computed in [3-013]. Three components are chosen: vertical force, side-side moment and fore-aft moment. Table 3-6 shows the relative difference between the two sets. In this table, the resultant damage equivalent moment has been obtained from the damage equivalent moments in the horizontal plane taken as its components. From the semi-floater concept to the INN WIND Jacket, it can be read substantial increases in vertical load and in fore-aft moment, whereas damage equivalent side-side moment of the two-bladed turbine is significantly lesser than that of the benchmark. This dichotomous relationship can be explained by high motions observed in the semi-floater in the wind direction compared to the motions realized in the case of jacket.

**Table 3-6 – Comparison of damage equivalent loads at interface for 25 years**

	Vertical Force (Fz)	Fore-aft Moment (Mx)	Side-side Moment (My)	Mres
2-bladed semi-floater	1336.6 kN	127830 kNm	57021 kNm	139971 kNm
INN WIND jacket	858.3 kN	99810 kNm	160150 kNm	188706 kNm
Relative difference	55.73 %	28.07 %	- 64.40 %	- 25.83 %

In addition, 1 Hz equivalent damage loads have been computed for each wind speed bin at the same structural locations. These loads have been obtained by:

$$L_1 = \left( \frac{\sum_i \sum_j N_{ij} S_{ij}^m}{N_{eq}} \right)^{1/m} = \left( \frac{\sum_i \sum_j n_{ij} S_{ij}^m}{T_s \times p} \right)^{1/m}, \quad (11)$$

with  $p = 54$  is the number of scenarios related to the given wind speed bin. The  $j$ -summation is done for all load range bins within a scenario  $i$ 's time series; and the  $i$ -summation is done for all scenarios related to the given wind speed bin.

Figure 3.8-1 to Figure 3.8-3 depict force and moment results separately. Forces exhibit a smooth increase with wind speed though slight bump appears toward 11 m/s to 13 m/s (around rated wind speed) especially for fore-aft forces, which are dominant compared to other forces. Similarly, fore-aft moments prevail to others and display higher and higher bumps around the same range (11 m/s to 13 m/s) as one goes from tower top to joint top.

The 1 Hz equivalent fatigue loads obtained at the interface have also been compared with those from [3-013]. The two result sets have been plotted in Figure 3.8-4. It can be observed that the semi-floater controller has managed to avoid load bumps at moderate wind speed domains as it is the case for jacket. Likewise the lifetime damage equivalent loads, vertical force and fore-aft moment are higher in semi-floater, whereas side-side moment has lesser values than those in jacket.

At small wind speeds (around 5 m/s), vertical force and fore-aft moment respectively have the same values in case of semi floater and of jacket. However, at high wind speeds greater values of tilt angle are observed for the semi-floater tower. Subsequently, the submerged portion of the buoyant chamber increases. As a result, more time varying contributions are added to vertical loads. Concurrently, sea states are more instable at they are wind speed dependent.

The large amplitude vibrations coupled with hydrodynamic effects generate higher variability to the vertical loads at high wind speeds. Explicitly, the coefficient of variation of the vertical load changes from about 0.25% at 5 m/s to about 1.60% at 25 m/s, i.e. about 6.4 times. That is why an growing trend is observed in the curves of Figure 3.8-4.

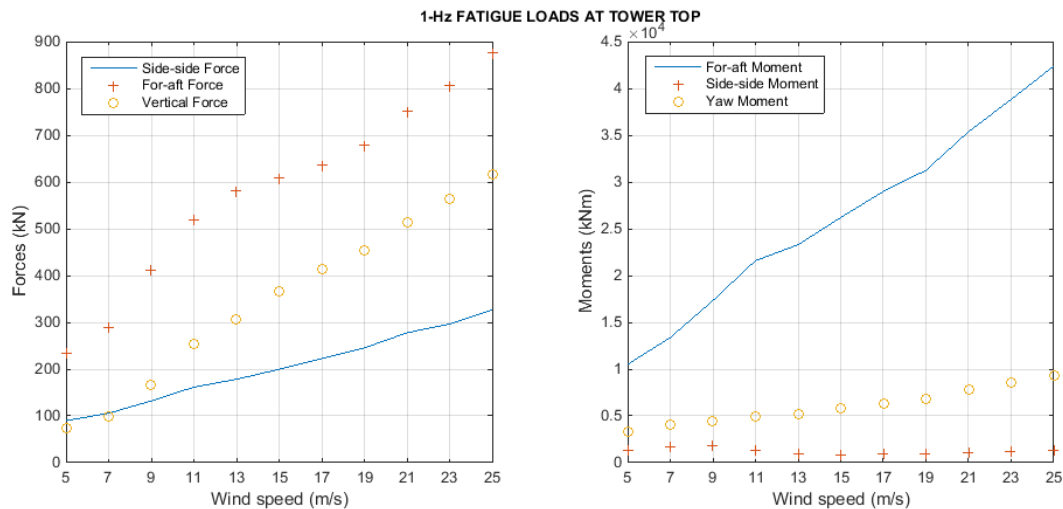


Figure 3.8-1 – 1 Hz damage equivalent load at tower top

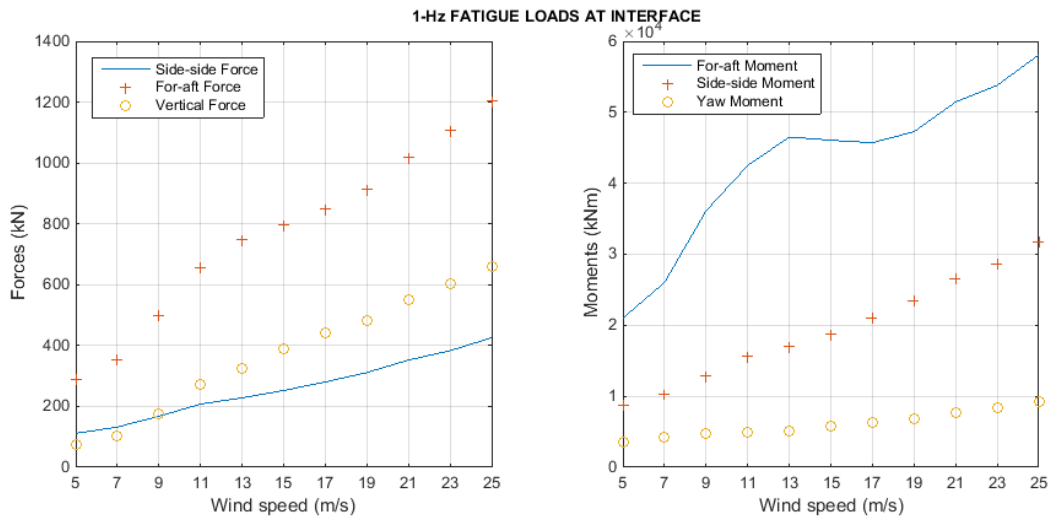


Figure 3.8-2 – 1 Hz damage equivalent load at interface

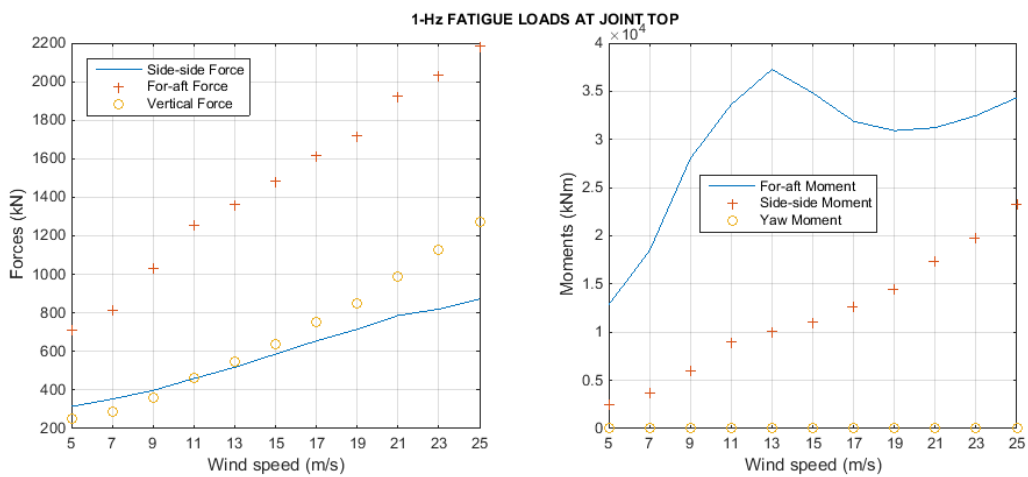


Figure 3.8-3 – 1 Hz damage equivalent load at joint top

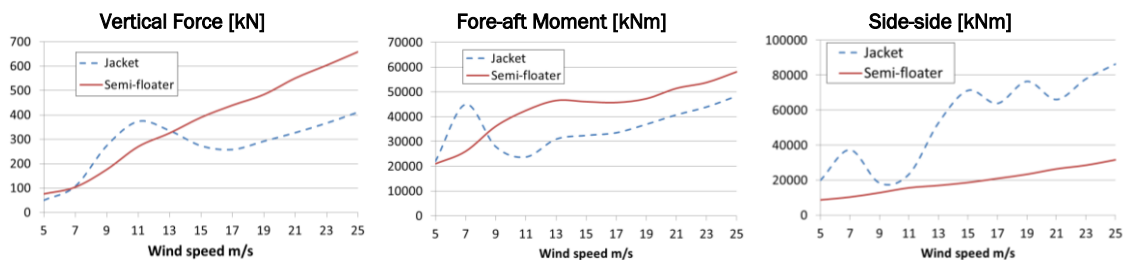


Figure 3.8-4 – Comparison of 1 Hz damage equivalent loads at interface

### 3.9 Advantages of the semi-floater concept

Two-bladed wind turbines generate load excitation at 1P and 2P frequencies, in this case [0.10 Hz, 0.16 Hz] and [0.20 Hz, 0.32 Hz]. This fact makes it difficult to avoid frequency resonance with fixed bottom structures whose frequencies generally lie between 1P and 3P. In the present study, the semi-floater support resolves this issue by setting the first whole structure eigen frequencies at about 0.068 Hz, lower than load excitation (wave and rotor) frequencies.

Consequently, this new concept presents damage equivalent loads comparable to those of three-bladed mounted on jacket. Most importantly, it achieves to reduce side-side fatigue loads to which aerodynamic damping is inefficient. In fact, for typical wind turbine structures, side-side vibrations are not damped by air viscosity as the contact surface is minimal. As a result, fatigue damage loads are generally severe in this direction. However, the semi-floater realizes about 65% of load reduction for lifetime fatigue load at interface. Similar reduction proportion is observed for 1 Hz fatigue damage equivalent load at 25 m/s. This reduction has been possible thanks to hydrodynamic damping, especially by the damping contribution of the mooring system, which acts along all directions.

Furthermore, the 1 Hz fatigue load curve as illustrated in Figure 3.8-4 do not show significant bumps around the rated wind speed. Considering that wind speeds around 12 m/s have higher occurrence, equivalent damage load bumps at that vicinity are to be avoided in order to minimize their negative effects. Once more, the semi-floater concept succeeds to reduce the loads at that wind speed range. Hence, lesser fatigue damage can be expected.

## 4 CONCLUSIONS

A two bladed 10 MW rotor was designed as installed on a semi floater platform and was successfully simulated in an aeroelastic software under normal operation in normal and extreme turbulence conditions. The rotor is similar to the reference 10 MW 3 bladed turbine, in the sense that the solidity is preserved, the rotor is upwind and the same airfoils are utilized. However the design driving excitation frequencies are P,2P, 4P etc, which required an innovative support structure.

The innovative support structure, which is a semi floater that is supported by an articulated joint at the sea floor, was designed in Task 4.13 and this was used herein with the 2 Bladed rotor. This is the first demonstration in the INN WIND.EU project of integration of multiple innovations into a single wind turbine concept. The system was tested with aeroelastic simulations validating the power performance, as well as the ultimate and fatigue design load limits. The system performs well under the simulated load cases and significant savings in the fatigue damage equivalent loads in the tower side to side direction was achieved. This is the main direction lacking aerodynamic damping and hence any 2P , 4P excitations in this direction would be detrimental to the structure.

By avoiding such resonant excitations, the turbine concept was shown to be fully functional and thereby at a TRL level 3 for 2 bladed wind turbine design at 10 MW scale. In Task 4.1,[3-04] the semi floater support structure was shown to only require 54% of the CAPEX as compared with the jacket structure. With the reduced side to side fatigue loads, even further reduction in Capex cost can be expected in relation to the jacket structure with a 2 bladed rotor.

As shown in Fig. 3.5.1 and Fig. 3.5.2, the power curve of the 2-Bladed turbine is nearly the same as the reference wind turbine and with nearly the same thrust, which therefore implies that the turbine capacity factor and the net wind farm efficiency will be the same as the reference wind turbine.

However with the reduced CAPEX cost of ~€3.5 million for the offshore sub structure including installation, the LCOE of a 500 MW wind farm based on INN WIND.EU deliverable D1.22 LCOE calculator is €85.6/MWH which is 7% lower than the LCOE for the reference 10 MW wind turbine installed on a jacket foundation. This is due to the low cost of the sub structure, which of course needs validation from industry. In summary, the innovative concept of the 2 Bladed rotor mounted on a semi-floater is shown to have significant benefits in fatigue load reduction of the sub structure and results in a reduction of LCOE by 7%.

## References

- [3-01] Bak C., Zahle F., Bitsche R., Kim T., Yde A., Henriksen L.C., Andersen P.B., Natarajan A., Hansen M.H.: “Design and performance of a 10 MW wind turbine”, J. Wind Energy, To be accepted.
- [3-02] INN WIND.EU Deliverable 4.1.2 – “Innovations on component level for bottom based structures (Interim Report)”, August 2014.
- [3-03] INN WIND.EU Deliverable 4.3.3 – “Innovative Concepts for Floating Structures”, August 2014
- [3-04] INN WIND.EU Deliverable 4.1.3 – “Innovations on component level (final report)”, August 2015
- [3-05] Larsen T.J., Hansen A.M.: “How 2 HAWC2, the user’s manual”, DTU Risoe 2014
- [3-06] IEC 61400-3: “Wind turbines – Part 3: Design requirements for offshore wind turbines Ed. 1.0”
- [3-07] INN WIND.EU Deliverable 4.3.1 – “Design Report – Reference Jacket”, October 2013
- [3-08] Hansen., M. H. & Henriksen, L. C.: “Basic DTU Wind Energy controller”, DTU Wind Energy.
- [3-09] Hansen, M. H. & Sønderby, I. B.: “Open- and Closed-Loop Aero-Servo-Elastic Analysis with HAWCStab2”, 2011
- [3-010] Hansen, M. O.: “Aerodynamics of Wind Turbines” s.l.:Earthscan. 2009
- [3-011] Larsen, T. J., Madsen, H. A., Thomsen, K. & Rasmussen, F., “Reduction of teeter angle excursions for a two-bladed downwind rotor”. Milan 2007
- [3-012] Skogestad, S. & Postlethwaite, I.: “Multivariable Feedback Control”. 2014
- [3-013] Madsen, H Aa, Bergami, L and Rasmussen, F: Deliverable 2.11 – “New aerodynamics rotor concepts specifically for very large offshore wind turbines”, September 2013
- [3-014] Bergami, L, Madsen, H Aa, Rasmussen, F: “A Two-Bladed Teetering Hub configuration for the DTU 10 MW RWT: loads considerations” . European Wind Energy Conference & Exhibition 2014